

Influence of Degree-Day Factor Variation on the Mass Balance of Glacier No. 1 at the Headwaters of Ürümqi River, China

Yuhuan Cui* (崔玉环), Baisheng Ye (叶柏生)

State Key Laboratory of Cryospheric Sciences, Cold and Arid Regions Environment and Engineering Research Institute, Chinese Academy of Sciences, Lanzhou 730000, China

Jie Wang (王杰)

School of Resources and Environmental Engineering, Anhui University, Hefei 230000, China

Youcun Liu (刘友存)

Key Laboratory of Water Resources and Environment, Tianjin Normal University, Tianjin 300387, China

ABSTRACT: The degree-day factor (DDF) is a key parameter in the degree-day model, and the variations in DDF have the significant effects on the accuracy of glacier mass balance modeling. In this study, Glacier No. 1 at the headwaters of Ürümqi (乌鲁木齐) River in China was selected, and the estimated DDF by stakes-observed mass balance and meteorological data from 1983–2006 was used to analyze the spatio-temporal variability of DDF and its influencing factors, such as climate condition, surface feature, and topography. Then, the ablations from the 1980s to 2000s were estimated using the degree-day model, and the ablation change from the 1980s to 2000s was divided into the changes caused by climate change and by the ice-surface feature. The following results were obtained: (1) The annual change in DDF for snow was not obvious, whereas that for ice increased, and the increasing trend on the lower glacier was more significant than that on the upper glacier because of decreased albedo caused by variations in ice-surface feature; (2) The DDF for ice clearly decreased with altitude by approximately 0.046 and 0.043 $\text{mm}\cdot\text{C}^{-1}\cdot\text{d}^{-1}\cdot\text{m}^{-1}$ on the east and west branches, respectively, and the DDF of the west branch was obviously larger than that of the east branch in the same altitude belt; (3) the changes in mass balance in the summers from the 1980s to 2000s were -391 and -467 mm on the east and west branches, respectively. Among the total changes, the components directly caused by climate change

were -193 and -198 mm, whereas those indirectly caused by ice-surface feature change were -198 and -269 mm on the east and west branches, respectively.

KEY WORDS: degree-day factor, mass balance, Glacier No. 1, climate change.

This study was financially supported by the National Natural Science Foundation of China (Nos. 41030527 and 41130368), the Global Change Research Program of China (No. 2010CB951404), and the Hundred Talents Program of the Chinese Academy of Sciences.

*Corresponding author: cuiyh@lzb.ac.cn

© China University of Geosciences and Springer-Verlag Berlin Heidelberg 2013

Manuscript received April 18, 2013.

Manuscript accepted September 15, 2013.

INTRODUCTION

The simulation and reconstruct in mass balance was important to glaciologists (Braithwaite and Zhang, 2000; Laumann and Reeh, 1993), and the degree-day model was applied to estimate the glacier ablation and

mass balance (Hock, 2005). Despite its simplicity, this model was shown to outperform the energy-balance model on a catchment scale, and was a powerful tool for melt modeling (Zhang et al., 2005; Liu et al., 1996; Braithwaite, 1995). The degree-day factor (DDF) was a key parameter in the degree-day model, and can simply describe the complicated process of energy transfer and transform on glaciers surface (Ohmura, 2001; Braithwaite and Zhang, 2000; Laumann and Reeh, 1993; Braithwaite and Olesen, 1989).

The degree-day approach was first introduced in research on an Alpine glacier by Finsterwalder and Schunk (1887). Since then, this approach has been used widely for estimation of snow/ice melting. Braithwaite and others (Braithwaite and Zhang, 1999; Braithwaite, 1995; Braithwaite and Olesen, 1989) used this approach to calculate melt on the Greenland ice sheet, showing that the DDF for ice is greater than for snow. Zhang et al. (2006) showed that the evident diversity of DDF existed among the glaciers of western China. With development of the degree-day model, the degree-day factor could no longer be regarded as constant, and variables, such as wind speed, relative humidity, solar radiation, vapor pressure etc., were included by some researchers to improve simulation accuracy (Arendt and Sharp, 1999; Schreider et al., 1997; Braithwaite and Olesen, 1993; Lang, 1968).

Under the influence of terrain conditions such as slope, aspect and shielding etc., the speed of ice and snow melt exhibits a tremendous spatial variability. Therefore, some authors (Arendt and Sharp, 1999; Hock, 1999; Schreider et al., 1997; Cazorzi and Fontana, 1996; Braithwaite and Olesen, 1993) have introduced the distributed degree-day model to improve simulation. Zhang et al. (2006, 2005) and Hock (2003) investigated positive degree-day factors on several typical glaciers in western China, such as the Keqicar Baqi Glacier. Their results clearly show that degree-day factor is subject to significant spatial and temporal variation from the influences of temperature, altitude, surface conditions etc.. Braithwaite (1995) calculated degree-day factor using the energy balance model, finding higher factor with lower albedo, under low temperature conditions.

The degree-day factors for ice and snow vary substantially under different climate conditions

(Braithwaite and Olesen, 1989). Based on the experiment of glacier melt runoff, Singh and Arora (2000) computed average degree-day factors for clean and dusty snow of 5.7 and $6.4 \text{ mm}\cdot\text{C}^{-1}\cdot\text{d}^{-1}$, respectively, the averages for clean ice and dusty ice were 7.4 and $8.0 \text{ mm}\cdot\text{C}^{-1}\cdot\text{d}^{-1}$. Liu et al. (1998) found a degree-day factor for snow of $3.1 \text{ mm}\cdot\text{C}^{-1}\cdot\text{d}^{-1}$, and between 5.1 and $10.1 \text{ mm}\cdot\text{C}^{-1}\cdot\text{d}^{-1}$ for ice. The degree-day factor varies spatiotemporally on the same glacier, because of the difference between snow and ice, and the uniqueness of the glacier surface.

Most glaciers in China have retreated the recent decades (Ding et al., 2006; Liu et al., 2006; Yao et al., 2004) and the retreated glacier lead to equilibrium-line altitude of glacier rise and the area of accumulation zone decrease. This article focuses on the variation of DDF and its influence on the glacier mass balance, using the stakes-observed mass balance by and meteorological data during 1983–2006. Therefore, the Glacier No. 1 at the headwaters of the Ürümqi River (UG1), with the ground measurement for more than 40 years, is chosen to study variations in glacier ablation and to feed-back to global climate warming. In the following, the variation of degree-day factor and its influence factors are analyzed using the mass balance observed by stakes, along with meteorological data from Daxigou Meteorological Station (DXG) near the glacier, then the glacier ablation in 1980s and 2000s are estimated by the degree-day model, and the change of ablation from 1980s to 2000s is divided into the change caused by climate change and the ice-surface feature change.

STUDY AREA

UG1 ($43^{\circ}06'N$, $86^{\circ}49'E$) is located in the eastern TianShan Mountains of northwest China. It is a northeast-facing valley glacier with two branches, east and west (Fig. 1). The two branches separated in 1993, owing to significant glacier shrinkage. In 2004, the total area of the glacier was approximately 1.708 km^2 . The east branch of the glacier is currently 1.101 km^2 in area, with a maximum elevation of $4\ 267 \text{ m a.s.l.}$; the west branch has approximately 0.607 km^2 , with a maximum elevation of $4\ 486 \text{ m a.s.l.}$

Field observations at UG1 have been taken since 1959, with interruptions during 1967–1979. Observa-

tions include glacier accumulation and ablation, equilibrium-line altitude (ELA), changes in glacier length and area, and hydro-meteorological data. Mass balance is calculated by contour maps of accumulation and ablation, using data from the permanent stake network on the glacier (about 45–80 stakes, in 8–9 rows) and from snow pits. Annual net accumulation, ablation and ELA have also been determined. The results indicate that the area of UG1 decreased by 0.242 km² from 1962 to 2004, which was 12.4% of the entire glacier area, and the decrease has rapid (Li et al., 2006).

Local meteorological data have been recorded from 1958 to 2011 at DXG, downstream from the glacier terminus (Fig. 1). During the period 1983–2006, the mean annual temperature and precipitation were -5.18 °C and 450.6 mm, respectively. Typically, 90% of the precipitation occurs between May and September.

DATA AND METHOD

Data

The basis of this research is mass balance of Glacier No. 1, observed approximately monthly from June through August during 1983–2006. We selected 27 stakes (7 rows and 15 stakes on the east branch, 6 rows and 12 stakes on the west, shown in Fig. 1) which represent different glacial surface characteristics. Since there is no meteorological data at the stake network, daily temperature and precipitation was extrapolated from the closest national meteorological station, DXG. The daily temperature at each stake was calculated from the daily DXG temperature and temperature gradients from different months (Table 1), using the following formula

$$PDD = \sum_t^n H_t \cdot (T_t - K_t(Z - Z_0)) \tag{1}$$

where PDD is the sum of positive air temperatures in an *N* days period; *T_t* is the daily mean air temperature at the meteorological station on day *t*; *H_t* is a logical

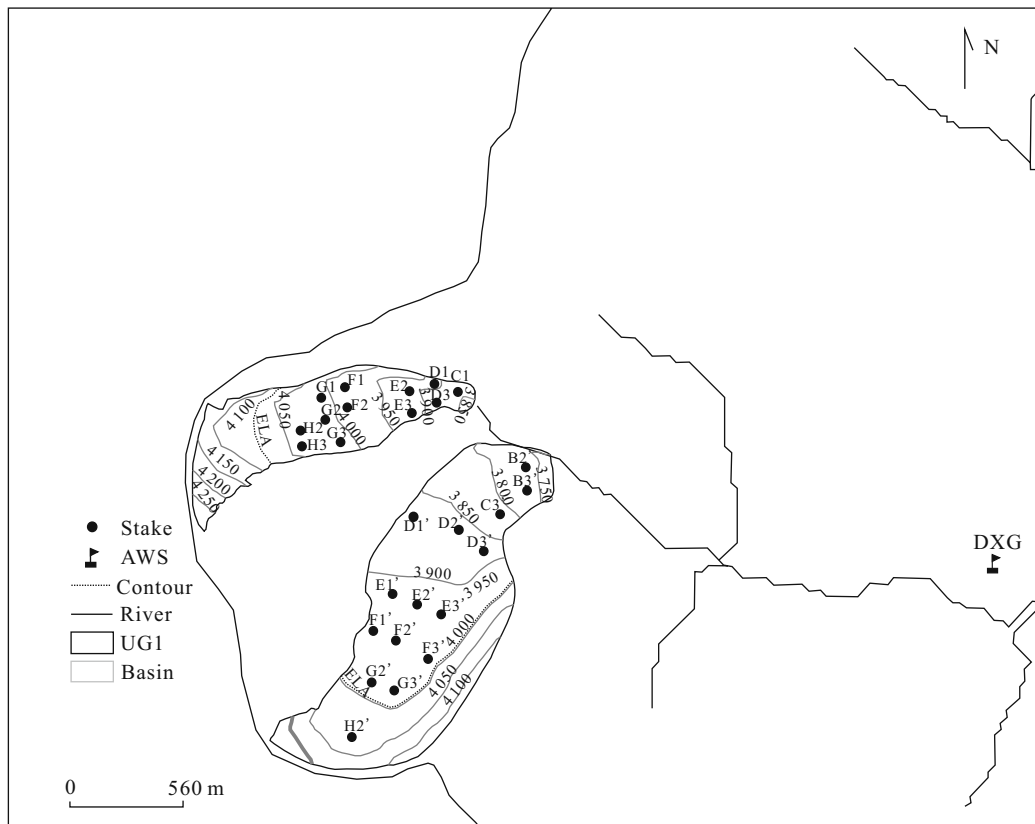


Figure 1. Locations of Glacier No. 1 at the headwaters of the Ürümqi River (UG1), and Daxigou Meteorological Station (DXG).

Table 1 Temperature gradient for each month

Month	1	2	3	4	5	6	7	8	9	10	11	12
Temperature gradients K_i (-°C/100 m)	0.298	0.319	0.409	0.527	0.600	0.529	0.600	0.571	0.584	0.423	0.326	0.266

variable, when $T_i \leq 0$, H_i was 0, else, H_i is 1; Z is the stake altitude in m; Z_0 is the altitude of the meteorological station in m; K_i is the temperature gradient in different months. Monthly precipitation at every stake was calculated from corrected precipitation at DXG (Ye, 1994) and a precipitation gradient of 22 mm/100 m (Yang et al., 1988), the formula used is

$$P_a = \sum_t^n P_{0t} + (Z - Z_0) \times 0.22 \quad (2)$$

where P_a is the precipitation at every stake in a period of N days and P_{0t} is the precipitation at DXG on day t .

The annual accumulated precipitation (P) and annual positive degree-day (PDD) were calculated using daily precipitation and temperature from DXG, during 1983–2006 (Fig. 2). The figure shows that P and PDD clearly increased during the study period, $5.66 \text{ mm}\cdot\text{a}^{-1}$ and $5.03 \text{ }^\circ\text{C}\cdot\text{a}^{-1}$ for P and PDD, respectively.

Methods

The degree-day factor (DDF) is the ratio of glacier ablation and PDD over the same period, and it has estimated using ablation and PDD at each stake in ablation period during 1983–2006, the formula is

$$\text{DDF} = M / \text{PDD} \quad (3)$$

where DDF is the degree-day factor and M is the depth of melt-water in an N day period.

M is calculated from the accumulation and the mass balance observed by stakes. The principal accumulation is from precipitation; therefore, the accumulation is substituted by the precipitation, assuming that all precipitation is in the solid state. The M is given by

$$M = P - B \quad (4)$$

where P is the precipitation (mm) in an N day period, and B is the mass balance (mm) in the same period.

DEGREE-DAY FACTOR AND SPATIO-TEMPORAL VARIATION Degree-Day Factor Calculated

The monthly DDF at every stake were calculated according to formulas (1)–(4), for summer periods from 1983–2006, and then we calculated the average DDF of B–H rows of stakes, for the sake of clearly shown in the figures (for example, DDF of row B' is the average DDF of stakes B2' and B3', with other row using the same method). DDF values for each month from 1983–2006 is shown in Fig. 3.

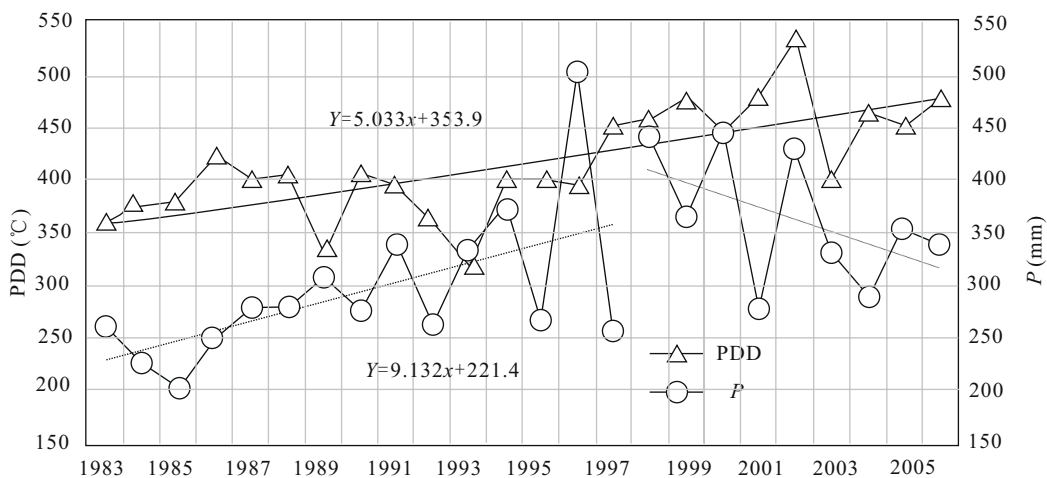


Figure 2. Variations in annual accumulated precipitation (P) and annual PDD (positive degree-day) at Daxigou meteorological station from 1983–2006.

The figure clearly shows that DDF of Glacier No. 1 presents an obvious variability both temporally and spatially. The DDF variation for different month is obvious, within a range on the east branch from 0.01 to 25.86 $\text{mm}\cdot\text{C}^{-1}\cdot\text{d}^{-1}$, and on the west branch from 0.03 to 24.29 $\text{mm}\cdot\text{C}^{-1}\cdot\text{d}^{-1}$. The biggest value for two branches both appears on the terminus of glacier in August 1993. There is the great diversity of DDF between the stakes due to the different melt rate. The trends of DDF also vary between the east and west branches, with a larger range of DDF changes.

Variation in Annual DDF in Summer

The annual degree-day factor (DDF) of the east and west branches of Glacier No. 1 at the headwaters of Ürümqi River in China from 1983–2006 (Fig. 4)

ranged from 1.12–14.30 $\text{mm}\cdot\text{C}^{-1}\cdot\text{d}^{-1}$ and from 0.98–13.84 $\text{mm}\cdot\text{C}^{-1}\cdot\text{d}^{-1}$, respectively. The DDF was largest on the terminus in 1993, which was caused by serious mass loss during the separation of the east and west branches, as mentioned above. On the other hand, the DDF was smallest in 1996, which was caused by high precipitation and low positive degree-day (PDD) during the year (Fig. 2). Before 1991, the DDF of the east and west branches did not obviously vary. After 1991, both the DDF values of the two branches had annual increasing trends, except in 1993. The DDF trends of the two branches spatially varied as follows: The DDF of the east branch clearly increased in the lower section (B', C', and D' rows) at a rate of 0.20 $\text{mm}\cdot\text{C}^{-1}\cdot\text{d}^{-1}\cdot\text{a}^{-1}$ and fluctuated with no evident trend in the middle and upper sections, but the DDF

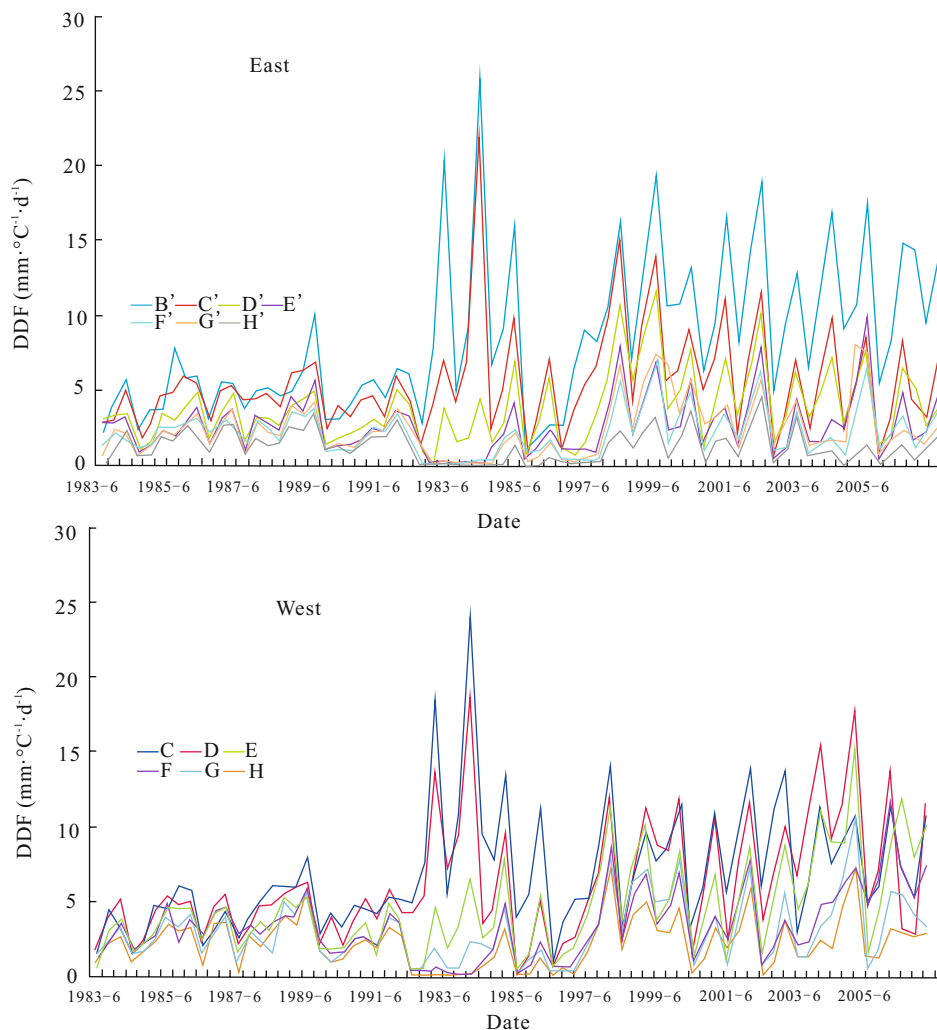


Figure 3. Variations in monthly DDF (Degree-day Factor) of the east and west branches of UG1 at each row of stakes in summer (DDF of row B' is the average DDF of stakes B2' and B3', and so on for other rows).

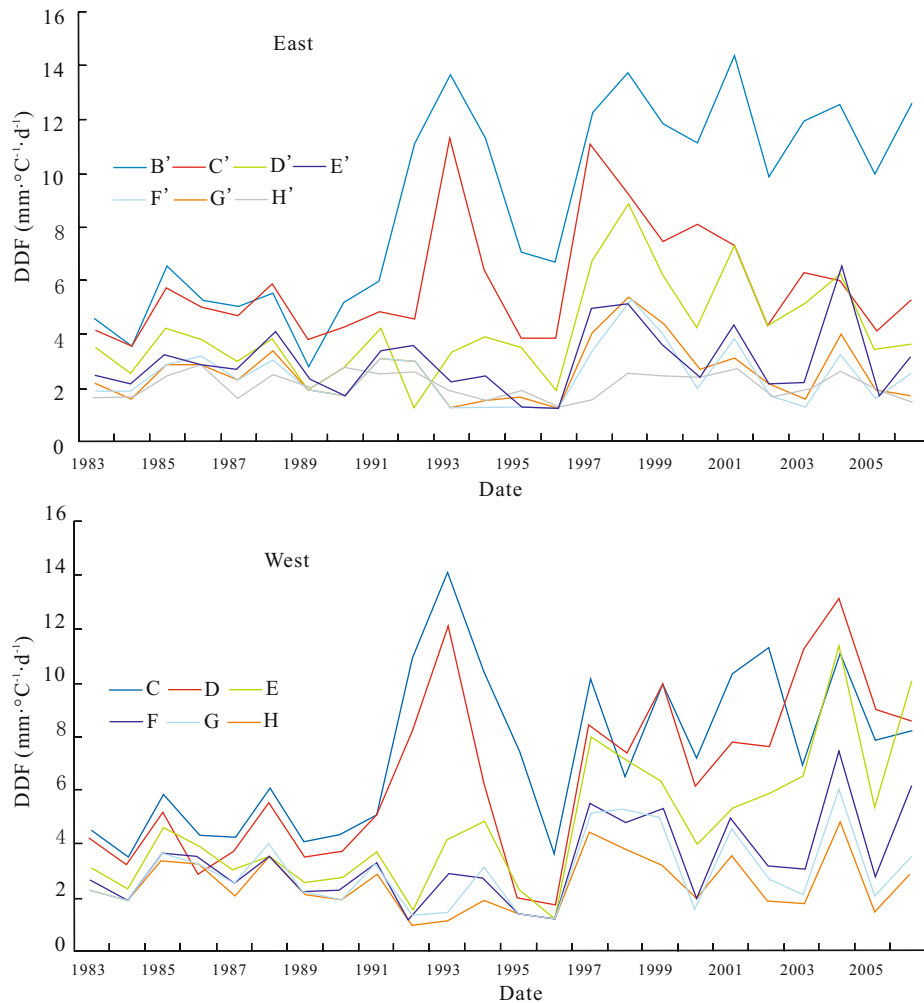


Figure 4. Variations in annual DDF of the east and west branches of UG1 at each row of stakes in summer (DDF of rows are defined as in Fig. 3).

of the west branch increased at an average rate of $0.15 \text{ mm}\cdot\text{C}^{-1}\cdot\text{d}^{-1}\cdot\text{a}^{-1}$ on all rows of stakes. The difference in the DDF values between the east and west branches was due to the higher equilibrium line altitude (ELA) of the west stake than that of the east stake and all other stakes below the ELA. Overall, the increase in DDF in the lower section was higher than that in the upper section possibly because of the difference in the melting rates of ice and snow. Therefore, the difference in the DDF values of snow and ice has been considered and estimated separately in this study.

Annual variations in the DDF for snow

The ELA on the east and west branches ranged from 3 905–4 140 m a.s.l. and from 3 975–4 240 m a.s.l from 1983–2006 (shown in Table 2). The stake H2' on the east branch, which was located at 4 050 m a.s.l., was the stake closest to the equilibrium line, and

thus, it was chosen for the investigation on the variations in the annual DDF for snow. As can be seen in Table 2, the elevation of H2' was above the ELA from 1983–1996, except for few years, and the ablation during this period was considered as melting snow.

Table 3 lists the DDF values at stake H2' from 1983–2006, where the values in the form of italics are considered as DDF values for snow. As can be seen in Table 3, the annual DDF change for snow ablation was not obvious, with an average value of $1.95 \text{ mm}\cdot\text{C}^{-1}\cdot\text{d}^{-1}$, but varied from 1.24–2.71 $\text{mm}\cdot\text{C}^{-1}\cdot\text{d}^{-1}$. The weak variations in the DDF for snow is a given contribution indicating that the stake H2' is located near the equilibrium line and perennially covered by snow, and its surface characteristics change were not obvious.

Table 2 Variations in ELA of the east and west branches of Glacier No. 1

Year	ELA-E (m)	E-H2' (m)	Year	ELA-E (m)	E-H2' (m)	Year	ELA-E (m)	E-H2' (m)
1983	3 937	4 073	1991	4 110	4 150	1999	4 095	4 170
1984	3 951	4 063	1992	3 918	4 032	2000	4 048	4 090
1985	4 081	4 112	1993	3 979	4 061	2001	4 115	4 153
1986	4 110	4 150	1994	4 037	4 079	2002	4 140	4 143
1987	3 980	4 070	1995	4 021	4 049	2003	4 066	4 089
1988	4 050	4 110	1996	3 947	4 025	2004	4 096	4 173
1989	3 976	3 976	1997	4 079	4 240	2005	4 045	4 071
1990	3 908	4 010	1998	4 055	4 138	2006	4 068	4 096

Table 3 Variations in DDF at H2' near the ELA (values in italics were chosen for the calculation of DDF for snow)

Year	DDF (mm·°C ⁻¹ ·d ⁻¹)	Year	DDF (mm·°C ⁻¹ ·d ⁻¹)	Year	DDF (mm·°C ⁻¹ ·d ⁻¹)
1983	1.70	1991	2.47	1999	2.37
1984	1.56	1992	2.53	2000	2.34
1985	2.42	1993	1.83	2001	2.71
1986	2.69	1994	1.57	2002	1.75
1987	1.59	1995	1.73	2003	1.91
1988	2.45	1996	1.24	2004	2.59
1989	1.99	1997	1.49	2005	1.93
1990	2.59	1998	2.40	2006	1.48

Annual variations in the DDF for ice

In the calculations of the DDF for ice (DDFi), the precipitation on the glacier was assumed to be in solid state and to provide the total source of the snowpack. In this study, the PDD used for glacier ablation was divided into two parts, namely, the PDD used to melt snow initially (PDDs) and the PDD for ice (PDDi) used to melt ice after the snowmelt. Based on these assumptions, the DDFi was calculated as follows

$$PDDs=P/DDFs \quad (5)$$

$$PDDi=PDD-PDDs \quad (6)$$

$$DDFi=(M-P)/PDDi \quad (7)$$

The DDFi from 1983–2006 was calculated using Formulas (5)–(7). Figure 5 shows the annual variations in DDFi. As can be seen in Fig. 5, the annual DDFi had an increasing trend, more significantly on the lower than on the upper glacier. Compared with Fig. 4, the annual variations in DDF in Fig. 5 shows a similar trend with that for the glacier, but the DDFi

was much larger than the DDF for the glacier, which implying that the melting rate of ice has a higher contribution to glacial melting rate, which can be related to the low albedo of ice. Dust accumulation or the darkening of snow or ice surfaces reduces surface albedo, leading to the higher absorption of solar radiation and increasing melt rate and greater meltwater. Using moderate resolution imaging spectroradiometer products, Wang et al. (2013) found that the albedo of Glacier No. 1 in summer decreased from 2000–2009. In the current study, the relationship between the surface albedo and the average DDFi on the UG1 from 2000–2006 (Fig. 6) was analysed, and the DDFi was found to increase with decreasing albedo during this period, which is consistent with previous findings on higher DDF with lower albedo at low-temperature glacial regions (Braithwaite, 1995).

Spatial Distribution of DDFi

The average DDFi values at each stake in summer from 1983–2006 were stratified into five levels at

equal intervals based on the calculated DDFi using formulas (5)–(7). Figures 7 and 8 show the spatial distribution map of DDFi and the variations in DDFi with altitude, respectively.

As can be seen in Fig. 7, the DDFi values of the east and west branches had obvious spatial variations from 2.19–15.93 $\text{mm}\cdot\text{C}^{-1}\cdot\text{d}^{-1}$, and from 3.79–13.35 $\text{mm}\cdot\text{C}^{-1}\cdot\text{d}^{-1}$, respectively. The largest DDFi value appeared on the east branch terminal, whereas the least DDFi value appeared at H2', which was closest to the ELA. Overall, the DDFi of the glacier decreased with altitude.

As can be seen in Fig. 8, the DDFi evidently decreased with altitude, and the decrease rates of the east and west branches were 0.046 and 0.043 $\text{mm}\cdot\text{C}^{-1}\cdot\text{d}^{-1}\cdot\text{m}^{-1}$, respectively. The decreasing trend of DDFi was much sharper on the lower glacier than on the upper glacier because ice-surface features change

with altitude. Dust accumulation or darkening of the ice surface became severe on the lower glacier when the glacier shrinking accelerated, reducing the albedo, causing more absorption of solar radiation, increasing melting rate and meltwater yield, and ultimately boosting DDFi. However, the dust accumulation or blackening of the ice surface had less influence on the upper glacier above the equilibrium line covered by snowpack, with a higher surface albedo, and consequently, a smaller DDFi.

The DDFi of the west branch was found to be obviously larger than that on the east branch within the same altitude belts. The difference in the DDFi values between the two branches was due to the diversity of solar radiation received by the glacier surface.

Variations in elevation, orientation (slope and aspect), and shadows cast affect the amount of

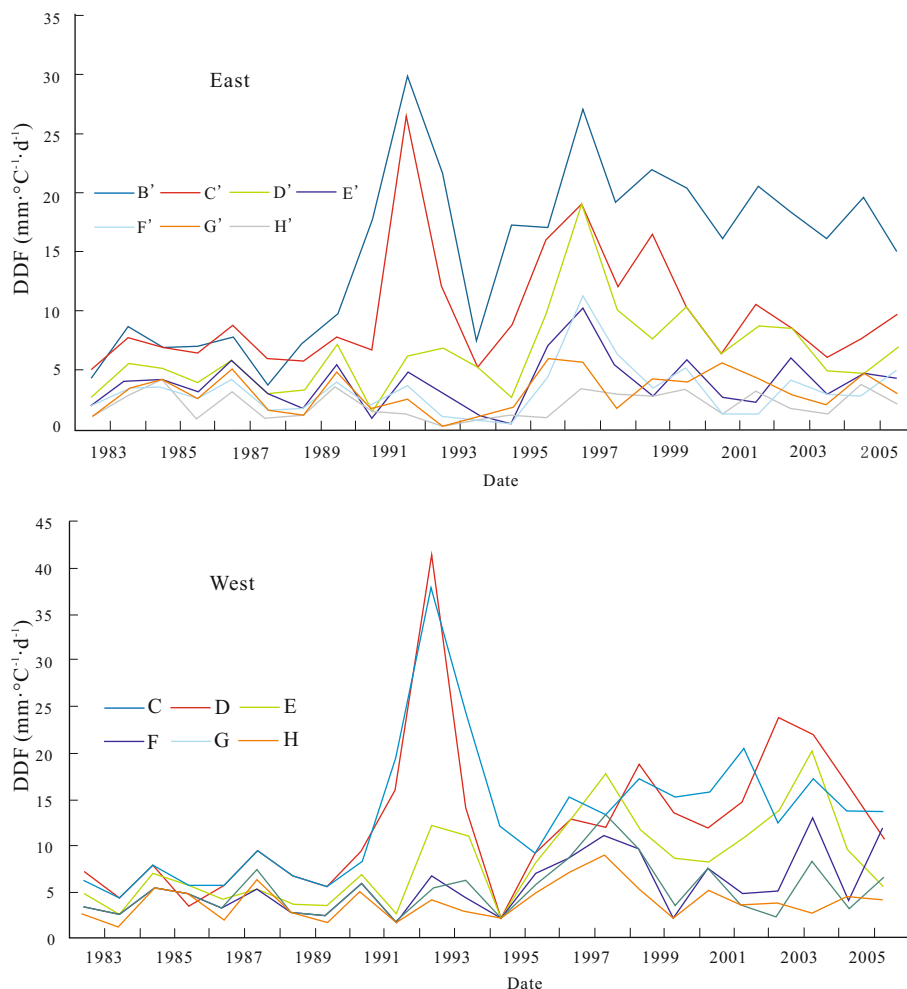


Figure 5. Variations in annual DDFi (DDF for ice) of the east and west branches of UG1 at each row of stakes during summer (DDFi of rows are defined as in Fig. 3).

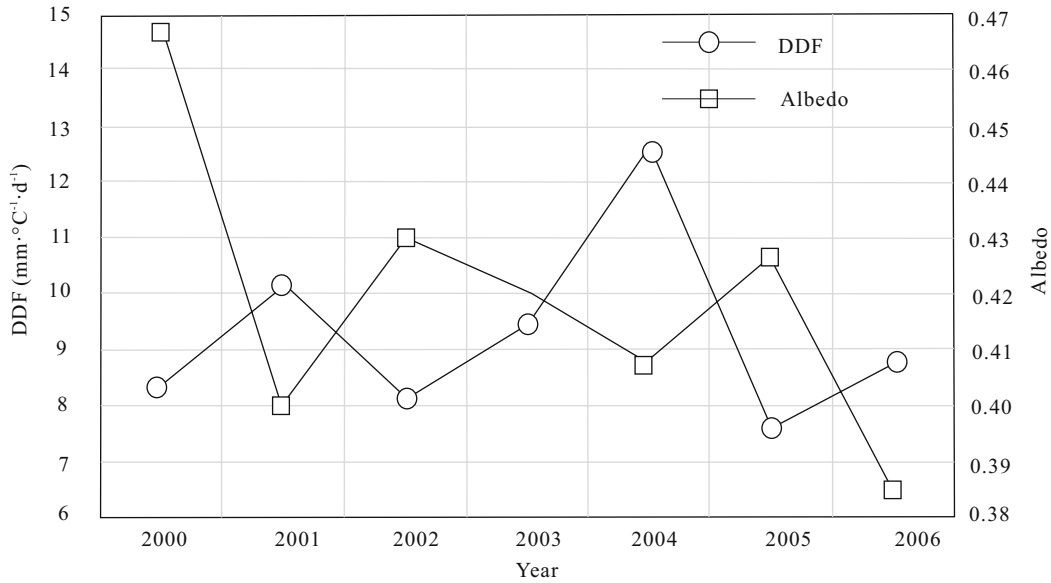


Figure 6. Variations in average DDFi (DDF for ice) and albedo of UG1 in the summers from 2000–2006.

income solar radiation at different stakes. In this study, the amount of income solar radiation was analyzed using the solar radiation analysis tools in the ArcGIS software. These tools account for site latitude and elevation, steepness (slope), and compass direction (aspect). The effects of shadows cast by surrounding topography enable the mapping and analysis of the effects of the sun over a geographic area for specific periods (Fu and Rich, 2002; Rich et al., 1995; Rich, 1990).

Figure 9 shows the relationship between the DDF and the global income solar radiation at each stake. As can be seen, the global income solar radiation of the west branch was obviously larger than that of the east branch. Moreover, the difference in the average solar

radiation between the west and east branches was 300 WH/m². This causes the more glacier ablation and the lower albedo at the west branch, the larger amount of absorbed solar radiation accelerates the glacier melting, and then leads to the larger DDF.

GLACIER ABLATION VARIATION

Changes in PDD and DDF can cause ablation change (ΔM), and thus, ΔM can be separated into $\Delta PDD \cdot DDF_0$ caused by climate change and into $\Delta DDF \cdot PDD$ caused by variations in ice-surface feature. The formulas are as follows

$$DDF = \Delta DDF + DDF_0 \tag{8}$$

$$PDD_0 = PDD - \Delta PDD \tag{9}$$

$$\begin{aligned} \Delta M &= DDF \cdot PDD - DDF_0 \cdot PDD_0 \\ &= (\Delta DDF + DDF_0) \cdot PDD - DDF_0 (PDD - \Delta PDD) \\ &= \Delta DDF \cdot PDD + \Delta PDD \cdot DDF_0 \end{aligned} \tag{10}$$

where ΔM is ablation change; DDF_0 and PDD_0 are initial values in 1980s (using the mean DDF and PDD from 1983 to 1989); DDF and PDD are values in 2000s under the conditions of climate change and surface feature variation (using the mean DDF and PDD from 2000 to 2006); ΔDDF and ΔPDD are the change values.

The changes in PDD and DDF were small from

1983 to 1989, and thus, the mean PDD and DDF values were chosen as PDD_0 and DDF_0 within this period, respectively. Under the conditions of climate change, the PDD and DDF values have changed since 1990, and thus, the mean DDF and PDD values from 2000–2006 were regarded as DDF and PDD values under the conditions of climate change and variations in surface feature. $\Delta DDF \cdot PDD$ can be regarded as the

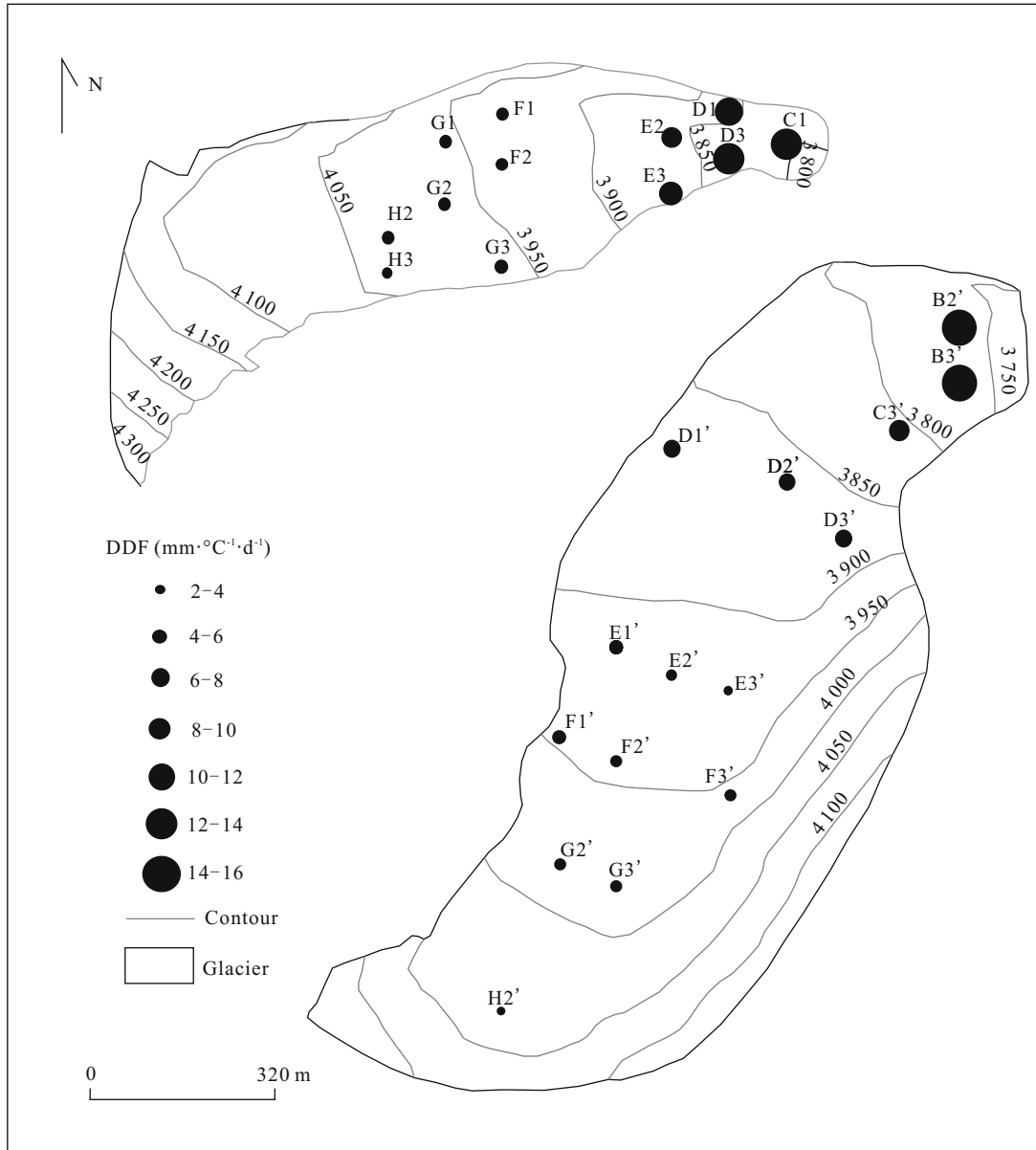


Figure 7. Spatial distribution of average DDFi on Glacier No. 1 from 1983–2006.

ΔM caused by variations in ice-surface features (ice surfaces with varying dirtiness) and $\Delta PDD \cdot DDF_0$ as the ΔM caused by climate change (including changes in air temperature and precipitation). The DDF_0 , PDD_0 , DDF , and PDD within different altitude belts were calculated using the average DDF value of the stakes within the same altitude belt, and the glacial ΔM caused by climate change and by variations in ice-surface feature was analyzed. Figure 10 shows the glacial ablation under the initial condition ($DDF_0 \cdot PDD_0$ in the 1980s), ΔM , and ablation caused by climate change ($\Delta PDD \cdot DDF_0$). As can be seen in

Fig. 10, ΔM decreased with altitude, and ΔM caused by climate change was not clearly fluctuating with altitude. These results imply that the ΔM caused by variations in ice-surface feature decreases with altitude, and approximately no ablation is found above the equilibrium line.

The ablation change from climate change and ice-surface variation has been estimated at every row in east and west branches (Fig. 10). The glacier ablation caused by climate change ($\Delta PDD \cdot DDF_0$) and by ice-surface feature variation ($\Delta DDF \cdot PDD$), both accounting for glacier ablation change (ΔM), are also

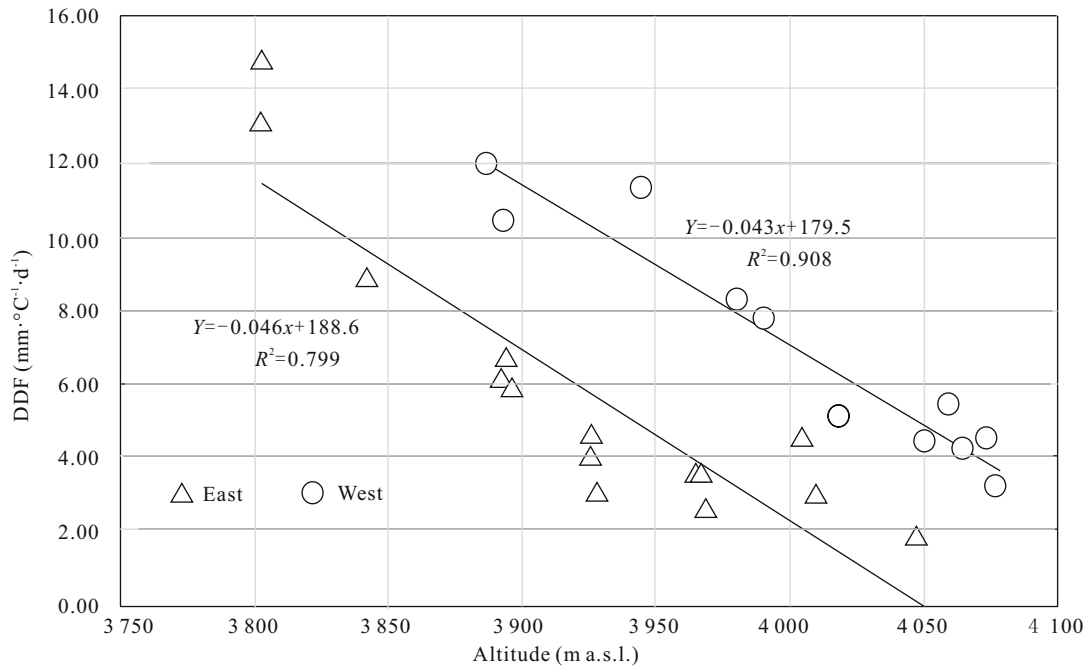


Figure 8. Variations in DDFi with altitude on Glacier No. 1.

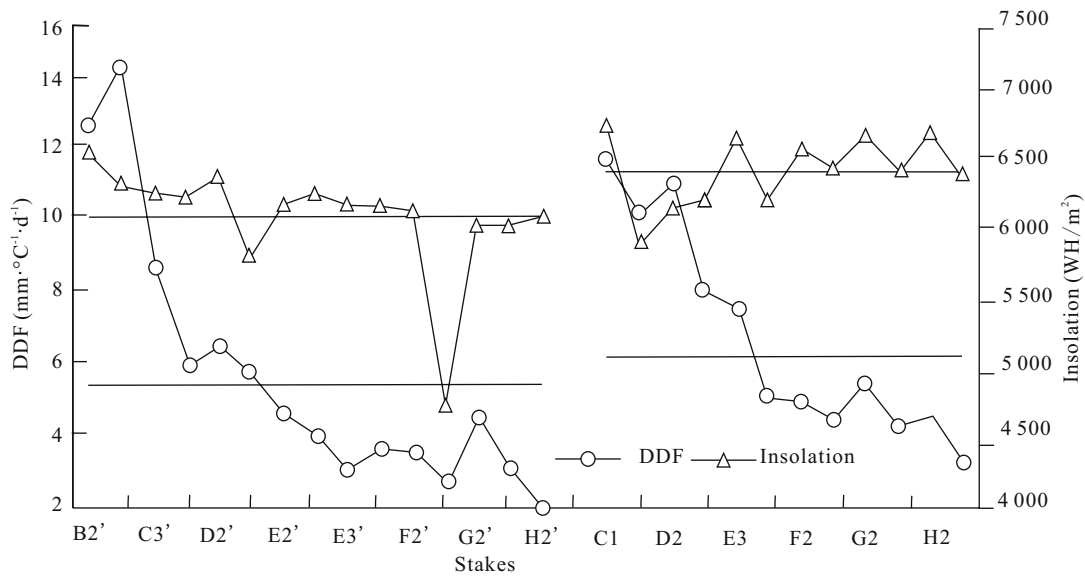


Figure 9. Variations in annual DDF and incoming solar radiation (insolation) at each stake on Glacier No. 1 in summer.

calculated and shown in Fig. 11. From the latter figure, it is evident that the percentages of $\Delta PDD \cdot DDF_0$ and $\Delta DDF \cdot PDD$, accounting for ΔM , represent the opposite trends with altitude. On the upper glacier (G and H rows), the total ablation change is mainly caused by climate change, about 91% and 76% for east and west branches, respectively, because ice-surface features change little. But on the lower glacier (B, C and D rows), the ablation change is affected by a combina-

tion of climate change and ice-surface feature variation together, and the influence of ice-surface feature variation on the total ablation is much more than that of climate changes, about 47% and 68% for east and west branches, respectively.

THE MASS BALANCE CHANGE

The glacier was divided into different altitude belts ($i=1 \dots n$) by 50 m intervals firstly, according to

ASTER GDEM with 30 meters resolution (provided by International Scientific Data Service Platform, Computer Network Information Center, Chinese Academy of Sciences). Then, the mean summer mass balance at each altitude belt in the 1980s and 2000s, and the summer mass balance after climate change at each altitude belt from 1980s to 2000s were calculated separately in the following research.

In this research, the mass balance in the accumulation and ablation zones was calculated respectively. The summer mass balance (B_s) in the accumulation zone was calculated using DDFs, PDDs, precipitation

gradient and DXG precipitation dataset. That in the ablation zone (B_i) was calculated using DDF_i , PDD_i , precipitation gradient and DXG precipitation dataset. B_s and B_i are calculated by formula (11). The summer mass balance for the entire glacier after climate change (B_t) was calculated using DDF_{s0} , DDF_{i0} and PDD, and precipitation (P) calculated, the calculated methods in accumulation and ablation zone are same as B_s and B_i .

$$B_s/i = P_i - PDD_s/i \cdot DDF_s/i \quad (11)$$

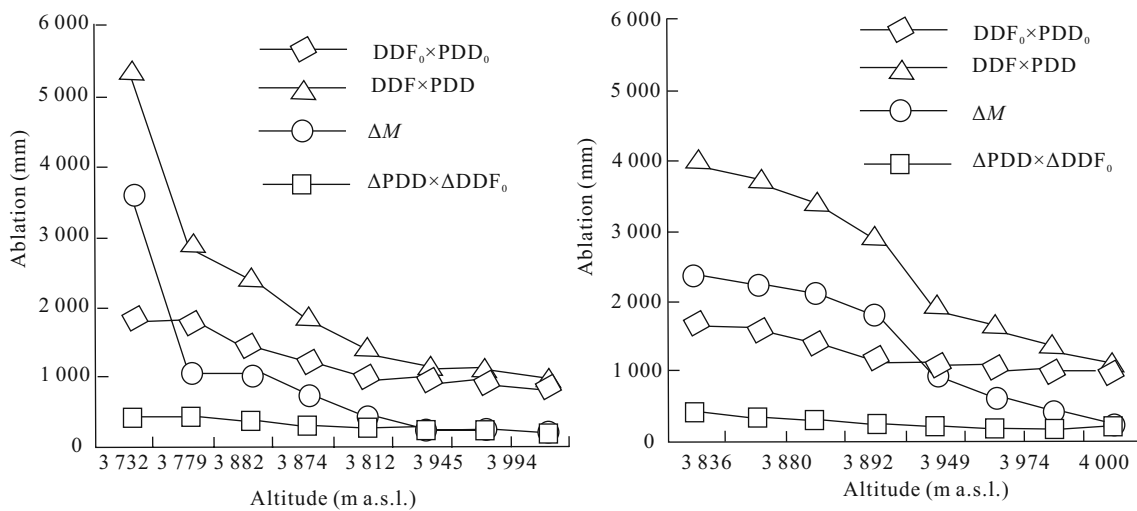


Figure 10. ΔM with altitude for different ice-surface features ($DDF_0 \times PDD_0$ is ablation in the 1980s, $DDF \times PDD$ is ablation in 2000s, ΔM is the total ablation change, and $\Delta PDD \times DDF_0$ is the ΔM caused by climate change).

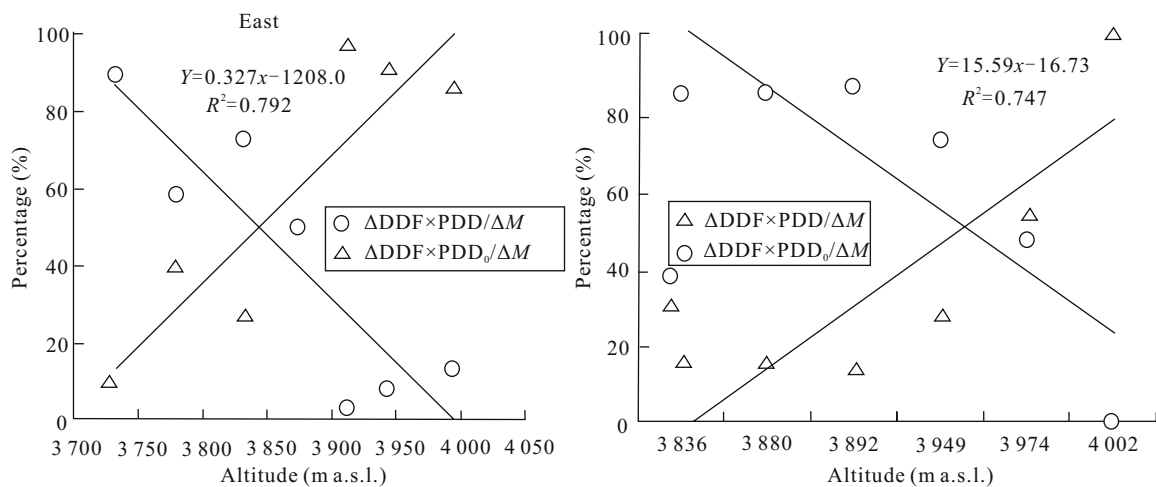


Figure 11. Contribution to total ΔM caused by climate change and variations in ice-surface with altitude of the east and west branches (ΔM is the total ablation change, $\Delta PDD \times DDF_0$ is the ΔM caused by climate change, and $\Delta DDF \times PDD$ is the ΔM caused by variations in ice-surface).

Where, $B_{s/i}$ is summer mass balance in the accumulation/ablation zone at i belt; P_i is the accumulation (precipitation) at i belt; $PDDs/i$ and $DDFs/i$ are the positive degree-day for snow/ice and degree-day factor for snow/ice at i belt.

Lastly, the average mass balance of glacier in 1980s and 2000s are denoted B_0 and B_z , and calculated by formula (11). The change of mass balance, and the change of mass balance caused by climate change is denoted ΔB and B_t , the formula is given by

$$\Delta B = B_z - B_0 \quad (12)$$

$$B_t = B_{ts} + B_{ti} \quad (13)$$

$$B_{ts/i} = \Delta P - \Delta PDDs/i \cdot DDF_{0s/i} \quad (14)$$

where B_{ts} and B_{ti} are the change of mass balance caused by climate change in the accumulation and ablation zone; ΔP and $\Delta PDDs/i$ are the change of precipitation and positive degree-day for snow/ice from the 1980 to 2000s; $DDF_{0s/i}$ is the degree-day factor for snow/ice in the 1980s.

According to the above formulas, the mass balance for east and west branches in 1980s, 2000s, the change of mass balance and the change of mass balance caused by climate change are calculated. The result shows that the variation of estimated mass balance over the last 20 years is -391 mm and -467 mm on the east and west branches, respectively. The respective differences directly caused by climate change for east and west branches are -193 mm and -198 mm, and the differences for east and west branch indirectly caused by ice-surface feature variation are -198 mm and -269 mm. This means that the contribution of mass balance change caused by climate change is 49% and 42% for the east and west branches, respectively. The respective contribution from ice-surface feature variation is 51% and 58%. Therefore, it can be concluded that climate change and surface feature variation are the two main reasons for the rapid shrinking of UG1.

CONCLUSIONS AND DISCUSSION

It is well known that most glaciers have been thinning and retreating in northwest China over the last 20 years due to climate warming (Shi et al., 2003). Therefore, it is very important to do the research on

glacier ablation, mass balance and their sensitivity to climate change, and DDF is an important parameter in mass balance modeling. Based on observed mass balance data at UG1 and weather data from DXG during 1983–2006, this research analyzes the spatiotemporal variability of DDF across the entire glacier firstly, and assesses the contributions of climate change and ice-surface feature variation to glacial mass balance changes by the method of degree-day model. The conclusions can be summarized as follows.

(1) The annual change of DDF for snow ablation is not obvious, with average value of $1.95 \text{ mm} \cdot \text{C}^{-1} \cdot \text{d}^{-1}$, while the annual change of DDF for ice ablation is increasing, with a more pronounced increase on the lower glacier than on its upper portions.

(2) DDF clearly decreased with altitude, the decreased trend is much sharper in the lower glacier than the upper, the decrease rate at east and west branches are 0.046 and $0.043 \text{ mm} \cdot \text{C}^{-1} \cdot \text{d}^{-1} \cdot \text{m}^{-1}$, respectively. It is also found that the DDF of west branch is larger obviously than that of east branch in same altitude belts.

(3) The mean mass balance change on the east and west branches during summer, from 1983–1989 to 2000–2006, are -391 mm and -467 mm, respectively. Of these respective changes, -193 mm and -198 mm are directly caused by climate change, and -198 mm and -269 mm are indirectly caused by ice-surface feature change. This means that the contributions of mass balance change from climate change are 49% and 42% for the east and west branches, respectively, and those contributed by ice-surface feature variation are 51% and 58%. Therefore, climate warming and the dirtier glacier surface are the main reasons for the rapid shrinking of Glacier No. 1 in the recent years.

As the key parameter of degree-day model, the accuracy of DDF would greatly influence the simulation of glacier mass balance. In the recent researches, DDF is considered as constant parameter or calculated by the measured mass balance at the limited points. The results of this research suggests that DDF varies obviously both in spatial and temporal, related to the local climate conditions, the changeable surface features and topography factors. Limited the existing observed points, the diversity of DDF within the same altitude could not be considered. Therefore, a new approach to calculate the DDF, containing the topogra-

phy factors (slope and aspect), is greatly needed to solve this problem.

REFERENCES CITED

- Arendt, A., Sharp, M., 1999. Energy Balance Measurements on a Canadian High Arctic Glacier and Their Implications for Mass Balance Modeling. *IAHS Publ.*, 256: 165–172
- Braithwaite, R. J., 1995. Positive Degree-Day Factor for Ablation on the Greenland Ice Sheet Studied by Energy Balance Modeling. *J. Glaciology*, 41(137): 153–160
- Braithwaite, R. J., Olesen, O. B., 1989. Calculation of Glacier Ablation from Air Temperature, West Greenland. In: Oerlemans, J., ed., *Glacier Fluctuations and Climatic Change*. Kluwer Academic Publishers, New York. 219–233
- Braithwaite, R. J., Olesen, O. B., 1993. Seasonal Variation of Ice Ablation at the Margin of the Greenland Ice Sheet and Its Sensitivity to Climate Change, Qamanrss Psermia, West Greenland. *J. Glaciology*, 39(132): 267–274
- Braithwaite, R. J., Zhang, Y., 1999. Modeling Changes in Glacier Mass Balance that May Occur as a Result of Climate Changes. *Geogr. Ann.*, 81A(4): 489–496
- Braithwaite, R. J., Zhang, Y., 2000. Sensitivity of Mass Balance of Five Swiss Glaciers to Temperature Changes Assessed by Tuning a Degree-Day Model. *J. Glaciology*, 46: 7–14
- Cazorzi, F., Fontana, G. D., 1996. Snowmelt Modeling by Combining Air Temperature and a Distributed Radiation Index. *J. Hydrology*, 181: 169–187
- Ding, Y. J., Liu, S. Y., Li, J., et al., 2006. The Retreat of Glaciers in Response to Recent Climate Warming in Western China. *Annals of Glaciology*, 43(1): 97–105
- Finsterwalder, S., Schunk, H., 1887. Der Suldenferner. *Zeitschrift des Deutschen und Oesterreichischen Alpenvereins*, 18: 72–89
- Fu, P., Rich, P. M., 2002. A Geometric Solar Radiation Model with Applications in Agriculture and Forestry. *Computers and Electronics in Agriculture*, 37: 25–35
- Hock, R., 1999. A Distributed Temperature Index Ice and Snowmelt Model Including Potential Direct Solar Radiation. *J. Glaciology*, 45(149): 101–111
- Hock, R., 2003. Temperature Index Melt Modeling in Mountain Areas. *J. Glaciology*, 282: 104–115
- Hock, R., 2005. Glacier Melt: A Review of Processes and Their Modeling. *Progress in Physical Geography*, 29(3): 362–391
- Lang, H., 1968. Relations between Glacier Runoff and Meteorological Factors Observed on and outside the Glacier. *IAHS Publ.*, 79: 429–439
- Laumann, T., Reeh, N., 1993. Sensitivity to Climate Change of the Mass Balance of Glaciers in Southern Norway. *J. Glaciology*, 39(133): 635–665
- Li, X. Y., Li, Z. Q., You, X. N., et al., 2006. Study of the Ice Formation Zones and Stratigraphy Profiles of Snow Pits on the Glacier No. 1 at the Headwaters of Urumqi River. *J. Glaciology and Geocryology*, 28(1): 37–44 (in Chinese with English Abstract)
- Liu, C. H., Xie, Z. C., Wang, C. Z., 1997. A Research on the Mass Balance Processes of Glacier No. 1 at the Headwaters of the Urumqi River, Tianshan Mountains. *J. Glaciology and Geocryology*, 19(1): 17–24 (in Chinese with English Abstract)
- Liu, S. Y., Ding, Y. J., Wang, N. L., et al., 1998. Mass Balance Sensitivity to Climate Change of the Glacier No. 1 at the Urumqi River Head, Tianshan Mts. *J. Glaciology and Geocryology*, 20 (1): 9–13 (in Chinese with English Abstract)
- Liu, S. Y., Ding, Y. J., Ye, B. S., et al., 1996. Study on the Mass Balance of the Glacier No. 1 at the Headwaters of the Urumqi River Using Degree-Day Method. In: *Proceedings of the Fifth Chinese Conference on Glaciology and Geocryology (Vol. 1)*. Gansu Culture Press, Lanzhou. 197–204 (in Chinese with English Abstract)
- Liu, S. Y., Sun, W. X., Shen, Y. P., 2006. Glacier Changes Since the Little Ice Age Maximum in the Western Qilian Shan, Northwest China, and Consequences of Glacier Runoff for Water Supply. *Journal of Glaciology*, 49(164): 117–124
- Ohmura, A., 2001. Physical Basis for the Temperature-Based Melt Index Method. *J. Appl. Meteorology*, 40: 753–761
- Rich, P. M., 1990. Characterizing Plant Canopies with Hemispherical Photography. In: Goel, N. S., Norman, J. M., eds., *Instrumentation for Studying Vegetation Canopies for Remote Sensing in Optical and Thermal Infrared Regions*. *Remote Sensing Reviews*, 5: 13–29
- Rich, P. M., Hetrick, W. A., Saving S. C., 1995. Modeling Topographic Influences on Solar Radiation: a Manual for the Solar Flux Model. Los Alamos National Laboratory Report LA-12989-M, Washington DC
- Schreider, S. Y., Whetton, P. H., Jakeman, A. J., et al., 1997. Runoff Modeling for Snow Affected Catchments in the Australian Alpine Region, Eastern Victoria. *J. Hydrology*,

200: 1–23

- Shi, Y. F., Shen, Y. P., Li, D. L., et al., 2003. An Assessment of the Issues of Climatic Shift from Warm-Dry to Warm-Wet in Northwest China. *China Meteorological Press*, Beijing. 4–97
- Singh, P. N. K., Arora, M., 2000. Degree-Day Factors for Snow and Ice for Dokriani Glacier, Garhwal Himalayas. *J. Hydrology*, 235: 1–11
- Wang, J., Ye, B. S., Cui, Y. H., et al., 2013. Spatial and Temporal Variations of Albedos on Nine Glaciers in Western China from 2000 to 2011. *Hydrological Processes*, doi:10.1002/hyp.9883
- Yang, D. Q., Jiang, T., Zhang, Y. S., et al., 1988. Analysis and Correction of Errors in Precipitation Measurement at the Head of Urumqi River, Tianshan. *J. Glaciology Geocryology*, 10(4): 384–400 (in Chinese with English Abstract)
- Yao, T. D., Wang, Y. Q., Liu, S. Y., et al., 2004. Recent Glacial Retreat in High Asia in China and Its Impact on Water Resource in Northwest China. *Science in China Series D: Earth Sciences*, 47(12): 1065–1075
- Ye, B. S., 1994. The Effect of Climatic Change on Water Resources in the Tianshan Mountains: [Dissertation]. Cold and Arid Regions Environmental and Engineering Research Institute, Chinese Academy of Sciences, Lanzhou. 49–50 (in Chinese)
- Zhang, Y., Liu, S. Y., Ding, Y. J., 2006. Spatial Variation of Degree-Day Factors on the Observed Glaciers in Western China. *J. Glaciology Geocryology*. 61(1): 89–98 (in Chinese with English Abstract)
- Zhang, Y., Liu, S. Y., Shangguan, D. H., et al., 2005. Positive Degree-Day Factor for Keqicar Baqi Glacier, South of Tianshan. *J. Glaciology Geocryology*, 27(3): 337–343 (in Chinese with English Abstract)